K-Shell Emission-Line Backlighter Source Optimization

James Tsay

Phillips Academy
Andover, MA

LLE Advisor: Reuben Epstein

Laboratory for Laser Energetics
University of Rochester
Rochester, NY
November 2008

Abstract:

X-ray backlighting is an important diagnostic technique used in laboratory experiments conducted on the OMEGA laser system. To obtain images of imploding cryogenic targets, short-pulse, high-energy laser beams are directed at a thin slab of solid material, creating plasma backlighters that project images of the target onto a photographic film. For ample image contrast, x-ray intensities of backlighters must exceed the continuum intensity of targets. Therefore, high-intensity spectral lines are desirable. The K-shell lines of He-like species hold particular interest due to the strength of their emission, as well as the sharpness of the line. Moreover, using Al as a backlighter source positions these He-α lines within a photon energy range where about 1/e of the light is absorbed by the target. PrismSPECT, a spectral analysis code simulating the atomic and radiative properties of plasmas, can reveal the effect of certain parameters on He-α line emission. With the program, the optimal temperatures were obtained for x-ray emissions of steady-state Al plasmas at given mass densities and thicknesses.

1. Introduction

Laser-powered fusion is becoming an increasingly significant point of interest in the scientific community. Ongoing research shows that, if fully realized, fusion can provide a sustainable, alternate form of energy devoid of harmful waste products like carbon dioxide. The most immediately promising nuclear reaction to be used for fusion power is the D-T fuel cycle, in which two hydrogen isotopes, deuterium and tritium, fuse together to produce an alpha particle, a neutron, and 17.6 MeV of kinetic energy shared between the two products,[1]

$$D + T \rightarrow {}^{4}He + n \quad . \tag{1.1}$$

This energy, converted to electricity, would be both clean and abundant. Large quantities of deuterium exist naturally in seawater, and tritium can be synthesized from lithium. Although the lithium supply is more limited than that of deuterium, it is still large enough to supply the world's energy demand for thousands of years.

At the University of Rochester's Laboratory for Laser Energetics (LLE), researchers are investigating fusion with the OMEGA laser system. The OMEGA laser beams are focused onto a target, a thin plastic shell coated on the inside with a layer of cryogenic DT, causing the target to implode. Measuring and evaluating these implosions employs diagnostic techniques like x-ray backlighting, which produces radiographs of the imploded cryogenic pellet. These imploded fusion targets emit spectral radiation across a broad range of photon energy. The backlighter must therefore "outshine" the miniature star-like implosion over a certain range of photon energies. Sharp, high intensity spectral lines can provide good picture contrast, and K-shell lines of He-like or H-like species are preferred. A thin slab of aluminum is chosen as a backlighter source because it positions these lines within a photon energy range where about 1/e of the light is absorbed by the target. This assures that variations in the attenuation due to the spatial structure of the imploded target will produce measurable image contrast. The Al forms a plasma, which radiates these He-α lines, among many others, isotropically. The radiation that travels towards and through the imploding target casts a shadow, projecting a replica image onto an image plate. For best results, the He-α lines should be "optimized" for maximum specific intensity by adjusting parameters such as temperature, mass density, thickness, and time.

2. Radiative Transfer

In order to optimize the emission of He-α and H-α lines in our Al backlighter, we must understand what happens when a laser beam strikes any given medium. In radiative transfer, the atomic processes of absorption, emission, and scattering affect the propagation of radiation through some medium. First, we introduce a fundamental quantity of a field of radiation: the specific intensity, I_ν.[2] The amount of radiant energy dE_ν in the frequency interval (ν, $\nu + d\nu$) transported across an area $d\sigma$, within solid angle $d\omega$, and during time dt is related to specific intensity by

$$dE_\nu = I_\nu \cos\theta \, d\nu \, d\sigma \, d\omega \, dt \quad , \tag{2-1}$$

with θ representing the angle between the outward normal of the area element $d\sigma$ and the direction of propagation of the radiation within the solid angle $d\omega$.[3] By optimizing the Al backlighter, we mean to maximize the spectral intensity of the He-α line, within a nominal photon energy range 1595 to 1600 eV, centered at the line energy. To describe the variation of intensity in a medium, we have the basic differential equation of transfer

$$\frac{dI_\nu}{ds} = \frac{\varepsilon_\nu}{4\pi} - \kappa_\nu I_\nu \quad , \tag{2-2}$$

where κ_ν is the absorption coefficient, ε_ν is the emissivity, and ρ is the density of the absorbing plasma in g cm^{-2}. Simply put, the equation of transfer states that as a beam of electromagnetic radiation propagates through a medium, it loses energy through absorption and gains energy through emission. The solution to this equation for the special case of a homogeneous medium is

$$I_\nu(s) = \frac{\varepsilon_\nu}{4\pi\kappa_\nu} + \left(I_\nu(0) - \frac{\varepsilon_\nu}{4\pi\kappa_\nu}\right)e^{-\kappa_\nu s} \tag{2-3}$$

for the specific intensity $I_\nu(s)$ at a distance s starting from an initial condition $I_\nu(0)$ at s=0.[4]

3. Einstein Coefficients and Spectral Line Formation

Two kinds of atomic spectral lines exist: emission lines and absorption lines. When an electron makes a transition from a particular, excited energy level to a lower energy state, it ejects a photon of a particular energy and wavelength, forming an emission line. When an electron makes the reverse transition, from a lower to a higher energy state, a photon becomes absorbed in the process, forming an absorption line. Depending on whether a photon is ejected or absorbed, a spectrum of such photons will show an emission spike or absorption drop at the associated wavelength. When the upper level is a continuum state, the absorption can occur over a broad range of energy. It is continuum absorption by the imploded target that forms the shadow in the radiographic image and continuum emission that competes with the emission-line backlighter by obscuring the shadow.

Three processes occur in the formation of a spectral line: spontaneous emission, stimulated emission, and absorption.[5] For each of these three processes, there is an associated Einstein coefficient, the probability of the associated process occurring. For example, we take the Einstein A_{ji} coefficient, which describes the rate at which the number density of atoms in level j, n_j, decays to a state i. The rate, then, at which spontaneous emission occurs is

$$\frac{\partial n_i}{\partial t} = A_{ji} n_j \quad , \tag{3-1}$$

where the subscript pair j and i denotes the transition of the electron from state j to lower state i. The Einstein coefficients B_{ji} and B_{ij} apply to stimulated emission and spectral absorption, respectively. Stimulated or induced emission refers to the process by which a photon at or very near the frequency of a certain transition induces an electron to make that transition, resulting in

the emission of an additional photon with the same phase, frequency, polarization, and direction as the original. The rate at which stimulated emission occurs is

$$\frac{\partial n_i}{\partial t} = B_{ji} I_\nu n_j \quad , \tag{3-2}$$

for the emitting transition from state j to state i.[3] The rate of both spontaneous and stimulated emission is proportional to the number of atoms in the excited state, n_j. Lastly, absorption occurs at the rate

$$\frac{\partial n_i}{\partial t} = -B_{ij} I_\nu n_i \ . \tag{3-3}$$

Like the rate of stimulated emission, the absorption rate is proportional to the radiation intensity at the frequency ν, as well as the number of atoms n_i in the initial state, but, in this case, the initial state is the state of lower energy, which is depleted by the absorption of a photon. Given the way the three Einstein coefficients, A_{ji}, B_{ji}, B_{ij}, are defined,[3] Eqs (3-2) and (3-3) have been written in terms of I_ν, the value of the specific intensity at the average frequency of the transition. This is a good approximation if the specific intensity does not vary significantly over the spectral width of the transition. Otherwise, an appropriate spectral average of the specific intensity is used.

The three Einstein coefficients, A_{ji}, B_{ji}, B_{ij}, are fixed probabilities, depending only on the properties of the associated atom. From this fact, we know that the relations we find between these coefficients at thermal equilibrium apply even if the state of the gas is not in equilibrium. At equilibrium, the net change in the number of excited atoms is zero, meaning opposing processes cancel each other out. Therefore, we have the relationship governing equilibrium between the two states i and j,

$$0 = A_{ji} n_j + B_{ji} I_\nu n_j - B_{ij} I_\nu n_i \quad . \tag{3-4}$$

If we assume Local Thermodynamic Equilibrium—that intensive parameters like temperature and mass density vary so slowly in space and time that one can assume thermodynamic equilibrium in some neighborhood about any given point—we know that, for a certain temperature, the population distribution of atomic states located near a given point will obey statistical distributions, such as the Maxwell-Boltzmann distribution, which describes the probability of finding a particle in certain energy states under conditions of equilibrium,

$$f(E) = A e^{-\frac{E}{kT}} \tag{3-5}$$

where A is a constant, E is the energy of the energy state, T is the absolute temperature, and k is the Boltzmann constant, with $k=1.381 \times 10^{-23}$ J/K = 8.62×10^{-5} eV/K. We also consider some non-equilibrium conditions where the simplicity of LTE does not apply.

4. Non-LTE Atomic Rate Equations

Unlike in LTE plasmas, where the derivation of population numbers is based on a purely local equilibrium, the atomic level populations of non-LTE plasmas depend on the surrounding radiation field, and on the time history of these populations. This requires a detailed consideration of the atomic processes that populate and de-populate the energy levels. We begin by introducing the basic time-dependent rate equation:

$$\frac{d}{dt} n_i = \sum_j n_j P_{ji} - n_i \sum_j P_{ij} \tag{4.1}$$

The leftmost expression indicates the change in the population of level *i* with time, the inner expression indicates the sum of the population processes into level *i* from all other levels *j*, and

the rightmost expression indicates the sum of the population processes out of level *i*. In the equilibrium case, the populating processes are balanced by the depopulating processes, and the populations do not evolve. This gives our second equation,

$$\sum_j n_j P_{ji} - n_i \sum_j P_{ij} = 0 \tag{4.2}$$

The rate coefficients P_{ij} represent sums of all relevant collisional and radiative processes, including ionization, recombination, excitation, and decay. The time-dependent rate equations of the form of Eq. (4.1) for all the significant atomic states are solved by the spectral analysis code PrismSPECT.

5. PrismSPECT

PrismSPECT is a spectral analysis code that simulates the atomic and radiative properties of plasmas.[6] By utilizing a database of the required atomic constants, such as oscillator strengths, atomic level energies, and transition energies, for the elements hydrogen through krypton, PrismSPECT can compute atomic level populations, ionization properties, and emission and absorption spectra for LTE and non-LTE plasmas.[7] As a result, we can easily investigate how properties of our plasma backlighter change with temperature, density, and plasma size.

6. Varying Parameters

We seek to understand the effect of independent parameters on the spectral intensity of our aluminum backlighter. To do so, we simply vary a parameter in question while holding the others constant within a PrismSPECT equilibrium simulation, looking to the atomic spectra between the photon energies of interest. We inspect the effects of temperature, mass density, and

plasma thickness on spectral intensities. Remember that we are interested in the maximum intensities for the Al K-α line, that is, the line centered around approximately 1600 eV.

Figure 6-1: Spectra from a 4 μm Al foil at 5.4 g/cm^3 density plotted for various temperatures.

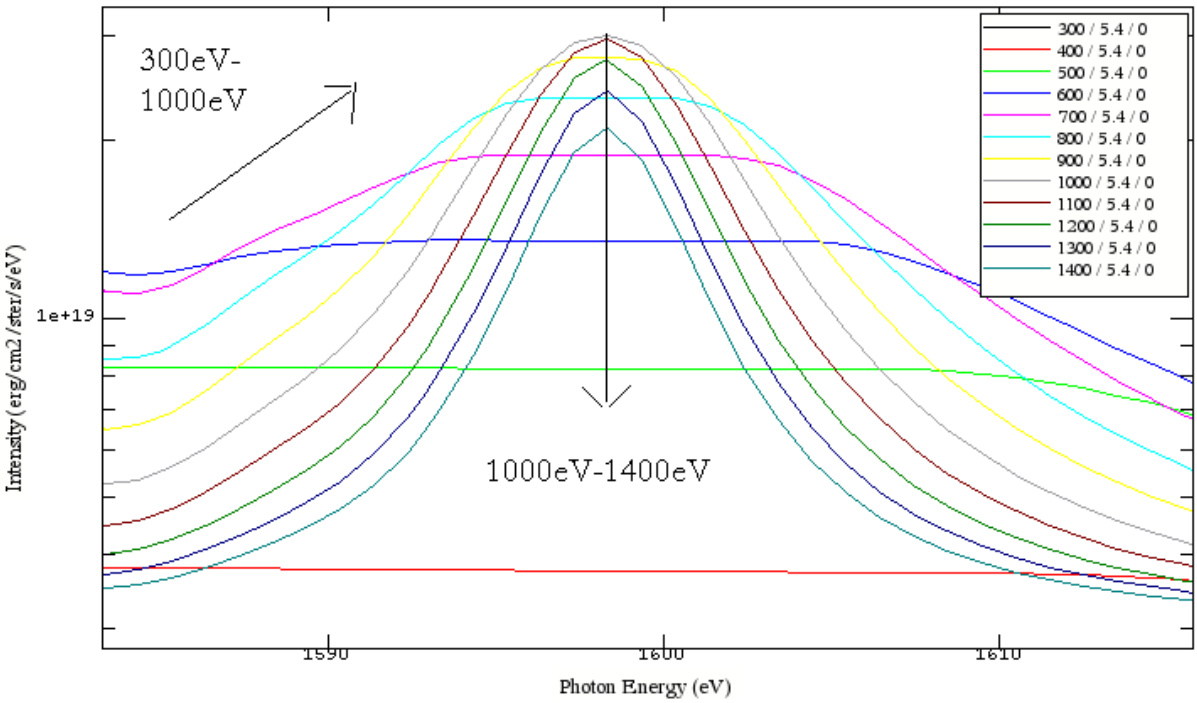

4 Micron Thickness

In Figure 6-1 we observe the effect of temperature on the K-α line for a sheet of Al at 4 μm thickness and a mass density of 5.4 g/cm^3, twice the density of cold Al. The temperatures are labeled in eV.

For temperatures between 300 eV to 1000 eV, we see an increase in the K-α line to a peak near 1 keV. However, as the temperatures continue to increase, the spectral intensities

actually decrease. This suggests that an optimal temperature exists for every given density and thickness.

Figure 6-2: Spectra from a 10 µm Al foil at kT=800 eV temperature plotted for various densities.

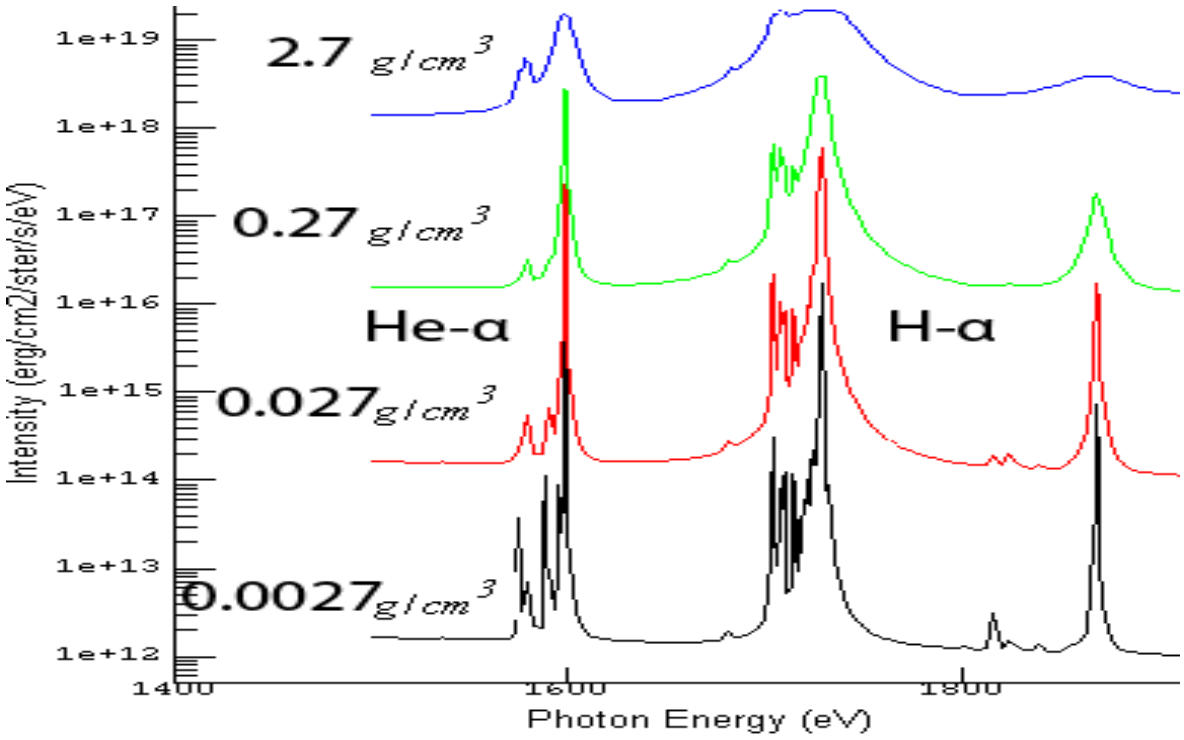

If we plot four more spectra at varying mass density, again, leaving all other parameters constant, we get spectra akin to those in Figure 6-2. The sheet is 10 µm thick, and the temperature is 800 eV. We display the starting mass density 2.7 g/cm^3, the density of aluminum at room temperature.

Notice that for every factor of ten with which the density decreases, the intensity decreases by a factor of one hundred. This observation makes sense, since ten times fewer

particles are in the aluminum plasma, and, at the same time, the density is reduced while keeping the foil thickness constant. The second factor of 10 reduction is the result of the reduced collisional excitation rate at this lower density. Conversely, denser aluminum emits higher intensity K-shell lines.

Figure 6-3: Spectra from Aluminum foils at 0.027 g/cm^3 density and at kT=400 eV temperature plotted for various foil thicknesses differing by factors of 10.

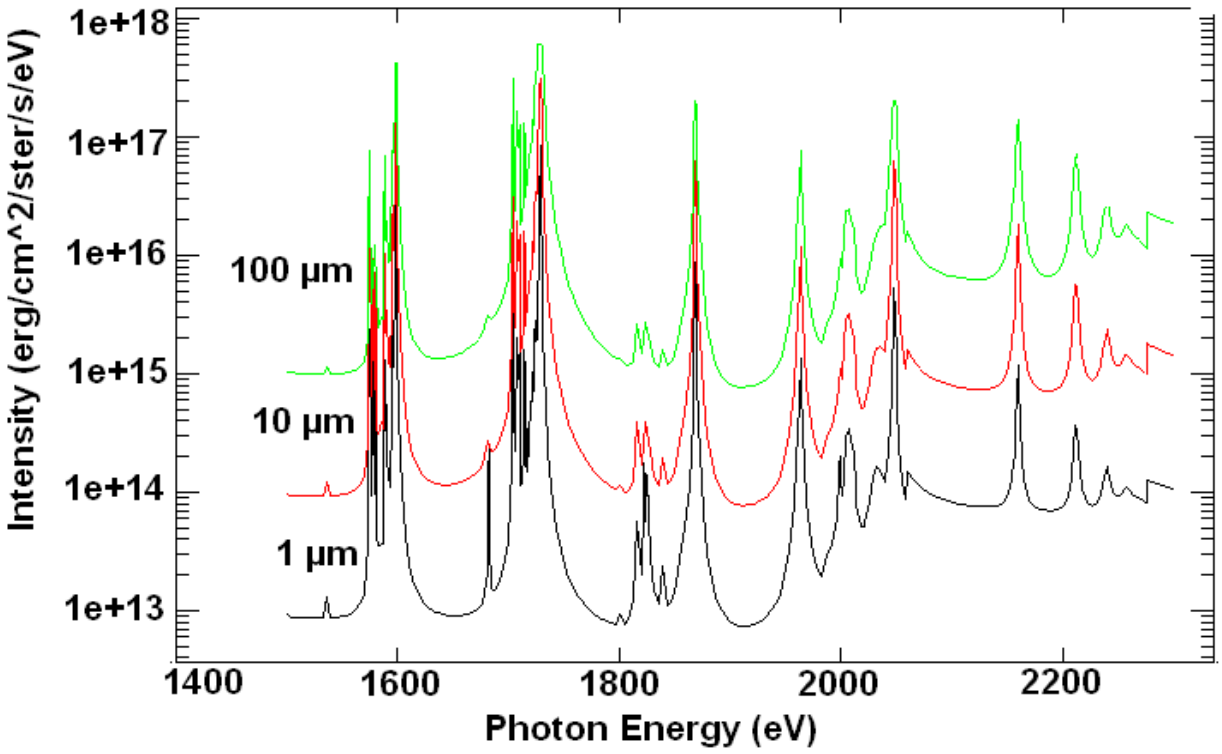

In Figure 6-3, we see three spectra at mass density 0.027 g/cm^3 and temperature kT=400 eV. Only thickness is varied. As the thickness of the aluminum increases by a factor of ten, so do the emitted spectral intensities. If density is constant and thickness is varied, then an increase in

volume corresponds to an increase in mass with a proportional change in the number of emitting atoms.

One might expect the spectra to vary with thickness as the previous density spectra varied with density, and since both series show the variation of spectra with the number of particles. Here, the spectral intensities do rise by a factor of ten with ten times the number of emitting particles and nothing more, because the number of emitters increases at constant density without increasing the excitation rate.

7. Optimized Temperatures for an Al K-α Backlighter

Under the range of conditions considered here, the spectral intensities appear to increase without bound for high densities and large thicknesses. So, in order to maximize the emitting intensities, we need only to find the optimal temperatures for given densities and thicknesses. We know that we can only elevate a given quantity of aluminum to emitting temperatures, so we concentrate on the foils usually used, those with thicknesses between 4 μm and 20 μm. Below, Figures 7-1, 7-2, and 7-3 each concern a foil of different thickness.

With PrismSPECT we can plot the integrated intensities of a spectrum between any two chosen photon energies. If we choose energies between 1597 and 1599 eV, we isolate the K-α line intensities, in which we are interested. We can plot these integrated intensities against the plasma temperature of our Al foil to find the optimal temperatures for K-α emission.

Figure 7-1: Spectral intensities integrated over the range of energy 1597-1599 eV centered at the Al He-α line plotted as functions of the temperature of a 4 μm thick Al foil.

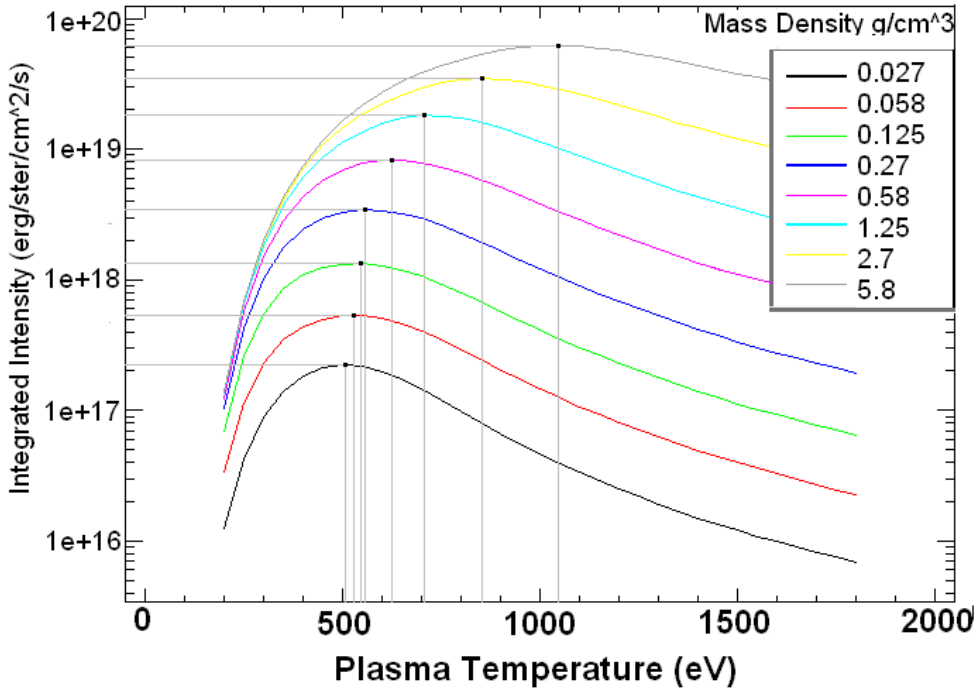

Figure 7-2: Spectral intensities integrated over the range of energy 1597-1599 eV centered at the Al He-α line plotted as functions of the temperature of a 10 μm thick Al foil.

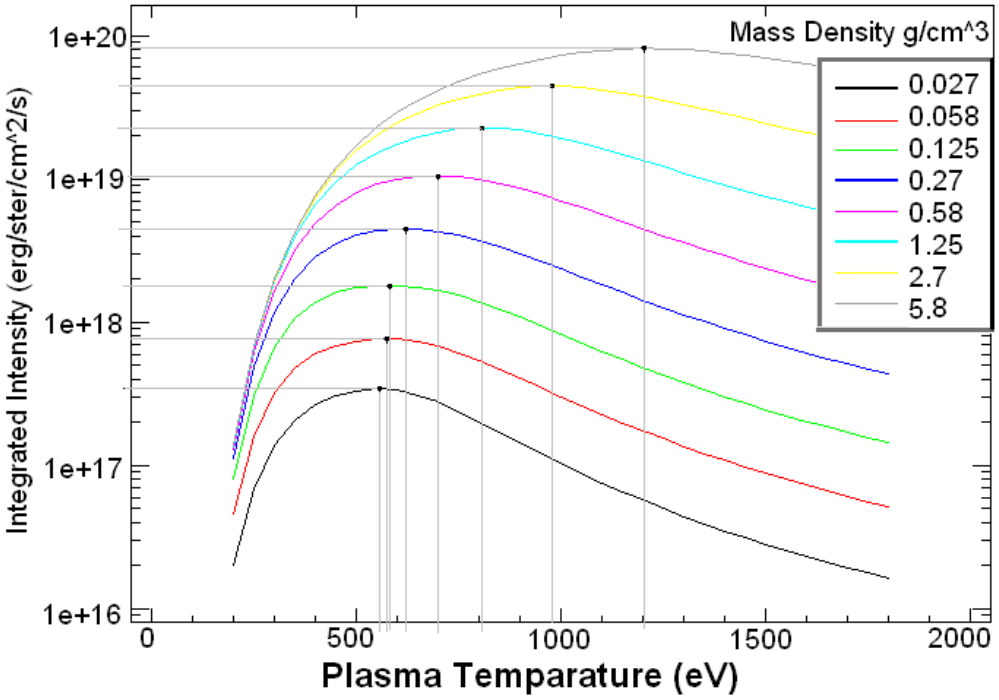

Figure 7-3: Spectral intensities integrated over the range of energy 1597-1599 eV centered at the Al He-α line plotted as functions of the temperature of a 20 μm thick Al foil.

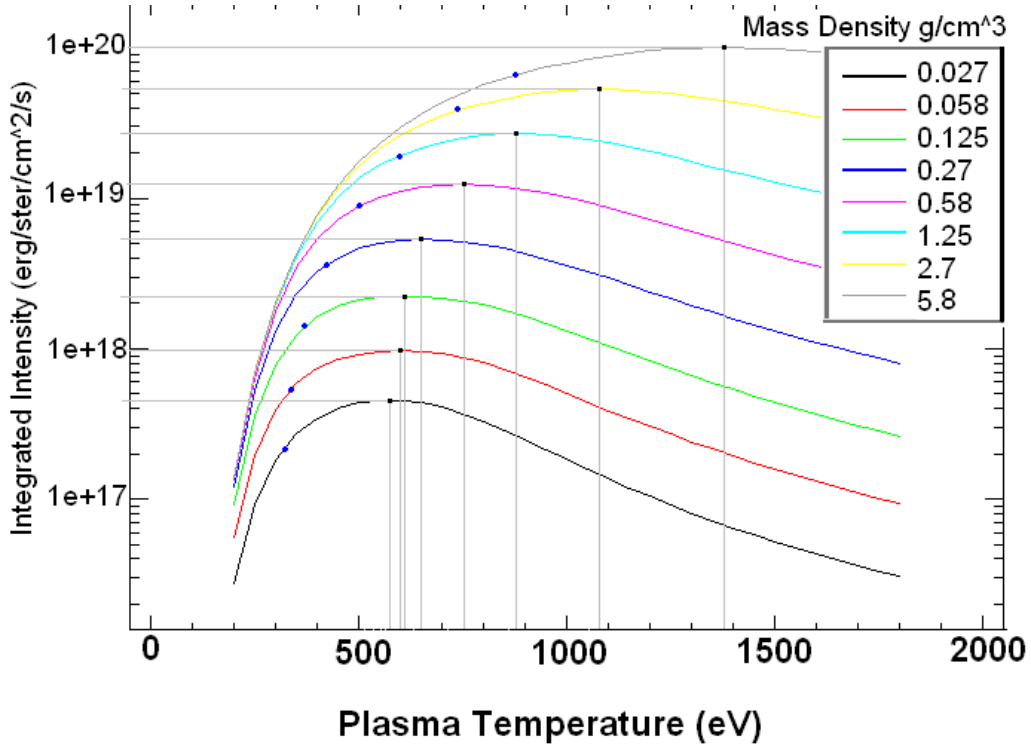

8. Conclusions

The study of Al H- α line intensities using PrismSPECT has thus far produced preliminary but useful results for optimizing emission-line backlighter sources. Within a plausible range of temperatures, densities, and foil thicknesses, the line intensity increases with the thickness of the foil at a given density and with the density of the foil at a given thickness. The limit on the amount of emitting material that can be brought to optimum emitting conditions will come from considerations such as the available backlight driver energy and the blackbody limit, which, thus far, has not been a significant limit in the cases considered here. While the line intensity increases with the source density, the optimum emitting temperature also increases with density, making increased demands on the backlight driver. Guided by the results obtained thus

far, future work would include using hydrodynamic simulations of backlight foils to determine the feasibility of obtaining optimum emitting conditions, including time-dependent atomic population calculations to verify that emitting conditions can be attained within the lifetimes of the hot plasmas.

Acknowledgements

I would like to thank my adviser Dr. Reuben Epstein for guiding me through my project, Dr. Stephen Craxton for accepting me into the program, and all of the other students at LLE's Summer Internship for High School Juniors for being great friends.

References

1. Craxton, R. S., R. L. McCrory, and J. M. Soures, *Progress in Laser Fusion*, Scientific American, Vol. 255, 68-79. August 1986.

2. An Introduction to Radiative Transfer, Annamaneni Peraiah, 1987 Cambridge University Press.

3. Foundations of Radiation Hydrodynamics, Dimitri Mihalas and Barbara Weibel-Mihalas, 1984 Oxford University Press

4. Stellar Atmospheres, Dimitri Mihalas, 1978 W H Freeman & Co.

5. Radiation Hydrodynamics, John I. Castor, 2004 Cambridge University Press.

6. PrismSPECT, Prism Computational Sciences, Inc., http://www.prism-cs.com/

7. Macfarlane, Joseph, et al. *PrismSPECT and SPECT3D Tools for Simulating X-ray, UV, and Visible Spectra for Laboratory and Astrophysical Plasmas*, American Physical Society, May 2003.